Phase diagram for a class of spin-half Heisenberg models interpolating between the square-lattice, the triangular-lattice and the linear chain limits

Zheng Weihong* and Ross H. McKenzie†
School of Physics, The University of New South Wales, Sydney, NSW 2052, Australia.

Rajiv R. P. Singh‡
Department of Physics, University of California, Davis, CA 95616
(February 1, 2008)

We study the spin-half Heisenberg models on an anisotropic two-dimensional lattice which interpolates between the square-lattice at one end, a set of decoupled spin-chains on the other end, and the triangular-lattice Heisenberg model in between. By series expansions around two different dimer ground states and around various commensurate and incommensurate magnetically ordered states, we establish the phase diagram for this model of a frustrated antiferromagnet. We find a particularly rich phase diagram due to the interplay of magnetic frustration, quantum fluctuations and varying dimensionality. There is a large region of the usual 2-sublattice Neél phase, a 3-sublattice phase for the triangular-lattice model, a region of incommensurate magnetic order around the triangular-lattice model, and regions in parameter space where there is no magnetic order. We find that the incommensurate ordering wavevector is in general altered from its classical value by quantum fluctuations. The regime of weakly coupled chains is particularly interesting and appears to be nearly critical.

PACS Indices: 75.10.-b., 75.10J., 75.40.Gb

I. INTRODUCTION

Quantum phases and phase transitions in two-dimensional Heisenberg models are of great current interest. [1] Following much experimental, theoretical, and numerical work, a fairly comprehensive and consistent picture has emerged for the ordered phases of unfrustrated Heisenberg models at zero and finite temperatures as well as for the quantum critical points separating them from the quantum disordered phases. [2,3] The case of frustrated Heisenberg models, potentially includes much richer phenomena and is relatively less understood. Here, the lattice models that have been studied the most are the square-lattice nearest and second neighbor interaction (or $J_{nn} - J_{nnn}$) model, where as a function of J_{nnn}/J_{nn}, the two and four sublattice colinear Neél phases are separated by a region of quantum disordered ground states. [4] Theoretical arguments and various numerical results suggest that this intermediate phase is spontaneously dimerized. Other models that have received considerable attention are the triangular-lattice and Kagome-lattice Heisenberg models. [5–7] The former appears to be magnetically ordered in the three-sublattice non-colinear pattern, whereas the latter almost surely has a non-magnetic ground state. The nature of the magnetically disordered phases and low energy excitations in these frustrated Heisenberg models are subjects of considerable interest.

Here we study a class of Heisenberg models that interpolate between the square-lattice, the triangular-lattice and the linear chain Heisenberg models. It can be defined in terms of a square-lattice of spin-half operators, with a nearest neighbor Heisenberg interaction J_2 and a second neighbor interaction J_1 along only one of the diagonals of the lattice. In the limit $J_1 \to 0$, we recover the square-lattice Heisenberg model. In the limit $J_2 \to 0$, the model reduces to decoupled spin-chains running along the diagonals of the square-lattice. For small J_2/J_1 the model consists of weakly coupled chains with frustrated interchain coupling. For $J_2 = J_1$, the model is exactly equivalent to the triangular-lattice Heisenberg model.

This model is of particular interest for at least two reasons. First, within a single Hamiltonian, it provides a way of interpolating between several well-known one and two dimensional models. One can study the role of frustration in going from one to two dimensions, [8] as well as the stability of commensurate and incommensurate magnetic order with respect to quantum fluctuations. [9] Second, the model is of direct relevance to the magnetic phases of various quasi-two-dimensional organic superconductors. It has been argued that this model should describe the spin degrees of freedom of the insulating phase of the layered molecular crystals, κ-(BEDT-TTF)$_2$X. [10] These materials probably have $J_1/J_2 \sim 0.3 - 1$. This ratio varies with the anion X and should vary with uniaxial stress applied within the layer along the diagonal. [11] A very slight variant on this model with $J_1/J_2 \sim 4$ has been proposed to describe the

insulating phase of θ-(BEDT-TTF)$_2$RbZn(SCN)$_4$ which has a spin gap. Recent studies of the associated Hubbard model on an anisotropic triangular lattice at half-filling suggest that the wave vector associated with the spin excitations determines the type of superconducting order. [12] Consequently, it appears that a good understanding of this Heisenberg model may be a pre-requisite to understanding organic superconductivity.

In this paper we study the zero-temperature phase diagram of this model by series expansions around various dimerized and magnetically ordered phases. Because of frustration, and large coordination number of the lattice, it would be difficult to get a comparable treatment of this model by any other numerical method. We will only consider $J_1 > 0, J_2 > 0$, that is both couplings are antiferromagnetic, which introduces frustration into the model. We find that the Neél order of the square-lattice Heisenberg model persists up to $J_1/J_2 \lesssim 0.7$, where it goes continuously to zero. It is interesting to note that Neél order exists beyond it regime of classical stability, providing an example of quantum order by disorder. [9] In the region $0.7 \lesssim J_1/J_2 \lesssim 0.9$, there is no magnetic order and the ground-state is dimerized in the columnar pattern. For larger values of J_1/J_2, there is incommensurate or spiral long-range order. Except for the triangular-lattice point ($J_1/J_2 = 1$), we find that the ordering wavevector is different from the classical Heisenberg model. At the triangular-lattice point, the dimer expansions indicate a magnetic instability at an ordering wavevector which coincides with the classical value. Furthermore, our Ising expansion series in this case reduce to previously derived series expansions directly for the triangular-lattice model. [5]

The region of large J_1/J_2 is very interesting and is not fully resolved by our series expansions. In the limit of small J_2, we have Heisenberg spin-chains coupled by frustrating zig-zag interactions. For just two such chains, this problem was studied by Affleck and White. [13] This zig-zag ladder has incommensurate spin correlations, a small gap and a spontaneous dimerization, which breaks the degeneracy of the weak zig-zag bonds but leaves the strong chain bonds equivalent. Our numerical results suggest that such a state is definitely not favored for the two-dimensional system. This is not hard to understand as such a broken symmetry phase can only have the strong bonds between every alternate pair of chains. We suggest three possible scenarios for this phase: (i) It has weak incommensurate spiral order, which vanishes rapidly (with a power greater than unity) as $J_2 \to 0$, (ii) This phase is dimerized along the strong J_1 bonds and has a spin-gap, (iii) The phase remains critical without any long-range order. The ground state energy obtained from the Ising expansions around a spiral phase and around a dimer state along the strong bonds remain nearly equal through much of this phase. In all three cases the system is close to being critical.

The elementary excitations of this phase and how they are connected to the excitations in isolated spin-chains should be very interesting to investigate. [14] The low-energy properties of models with non-collinear order are described by the SO(3) non-linear sigma model. [15,16] In the quantum disordered phase of this model the elementary excitations are deconfined spin-1/2 objects, or spinons, [17,3] in contrast to the magnons or spin-one triplets that are the elementary excitations in most two-dimensional antiferromagnets. Thus, this model, with spiral classical order provides us with candidate systems to look for spinon excitations.

The plan of the paper is as follows. In Sec. II we discuss the model and the various series expansions that are carried out. In Sec. III we discuss the results for the phase diagram, the ground state energy, the excitation spectra and the correlation functions of the model. Finally, in the last section we present our conclusions and discuss some future directions.

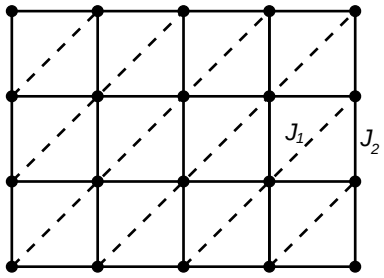

FIG. 1. The anisotropic triangular lattice with coupling J_1 and J_2.

II. SERIES EXPANSIONS

The Heisenberg antiferromagnet on an anisotropic triangular lattice is equivalent to the Heisenberg antiferromagnet on a square lattice with nearest neighbor interactions and one of diagonal next-nearest neighbor interactions as shown in Fig. 1. The Hamiltonian is:

$$H = J_1 \sum_{\langle in \rangle} \mathbf{S}_i \cdot \mathbf{S}_n + J_2 \sum_{\langle ij \rangle} \mathbf{S}_i \cdot \mathbf{S}_j \qquad (1)$$

where $\langle ij \rangle$ means pairs of nearest neighbors and $\langle in \rangle$ means one of diagonal next-nearest neighbor pairs, as illustrated in Fig. 1. We denote the ratio of the couplings as y, that is, $y \equiv J_1/J_2$. In the present paper, we study only the case of antiferromagnetic coupling, where both J_1 and J_2 are positive. In the limit $J_2 = 0$, the model is equivalent to decoupled one-dimensional Heisenberg chains. In the limit $J_1 = 0$, the model is equivalent to the two-dimensional square-lattice Heisenberg model. For $J_1 = J_2$, the model is equivalent to the Heisenberg model on a triangular lattice.

Let's discuss the classical ground state of this system: If we assume $\langle \mathbf{S}_i \rangle$ lies in the $x - z$ plane, we can rotate

all the spins related to a reference spin so we have a ferromagnetic ground state. The classical ground state of this system has nearest neighbor spins differ by an angle q, and spin joined by a diagonal bond differ by $2q$, where q is

$$q = \begin{cases} \pi, & J_1 \le J_2/2; \\ \arccos(-J_2/2J_1), & J_1 > J_2/2. \end{cases} \quad (2)$$

The angle q as a function of $J_1/(J_1+J_2)$ is shown as the solid curve in Fig. 2.

After this rotation, the transformed Hamiltonian is

$$H = H_1 + J_1 H_2 + J_2 H_3, \quad (3)$$

where

$$\begin{aligned} H_1 &= J_1 \cos(2q) \sum_{\langle in \rangle} S_i^z S_n^z + J_2 \cos(q) \sum_{\langle ij \rangle} S_i^z S_j^z \ , \\ H_2 &= \sum_{\langle in \rangle} S_i^y S_n^y + \cos(2q) S_i^x S_n^x + \sin(2q)(S_i^z S_n^x - S_i^x S_n^z) \quad (4) \\ H_3 &= \sum_{\langle ij \rangle} S_i^y S_j^y + \cos(q) S_i^x S_j^x + \sin(q)(S_i^z S_j^x - S_i^x S_j^z) \ . \end{aligned}$$

We have studied this system by using linked-cluster expansion methods at zero-temperature including Ising expansions, and dimer expansions about two different dimerization patterns. The linked-cluster expansion method has been previously reviewed in several articles [18–20], and will not be repeated here. Here we will only summarize the expansion methods used, and the results derived from them will be presented. The series coefficients are not given here, but are available upon request. Previous studies using these methods have agreed quantitatively with other numerical studies (including quantum Monte Carlo and exact diagonalization) for unfrustrated spin models. For frustrated two-dimensional models, both the Monte Carlo and the exact diagonalization methods face problems (due to the minus signs in case of the former and tremendous variations with size and shapes of the clusters in case of the latter). Thus, we believe, it would be difficult to get a comparable numerical treatment of this strongly frustrated model by other numerical methods.

A. Ising Expansions

To construct a $T = 0$ expansion about the classical ground state for this system, one has to introduce an anisotropy parameter λ, and write the Hamiltonian for the Heisenberg-Ising model as

$$H = H_0 + xV \ , \quad (5)$$

where

$$\begin{aligned} H_0 &= H_1 - t \sum_i S_i^z \ , \\ V &= J_1 H_2 + J_2 H_3 + t \sum_i S_i^z \end{aligned} \quad (6)$$

The last term of strength t in both H_0 and V is a local field term, which can be included to improve convergence. The limits $x = 0$ and $x = 1$ correspond to the Ising model and the isotropic Heisenberg model, respectively. The operator H_0 is taken as the unperturbed Hamiltonian, with the unperturbed ground state being the usual ferromagnetically ordered state. The operator V is treated as a perturbation.

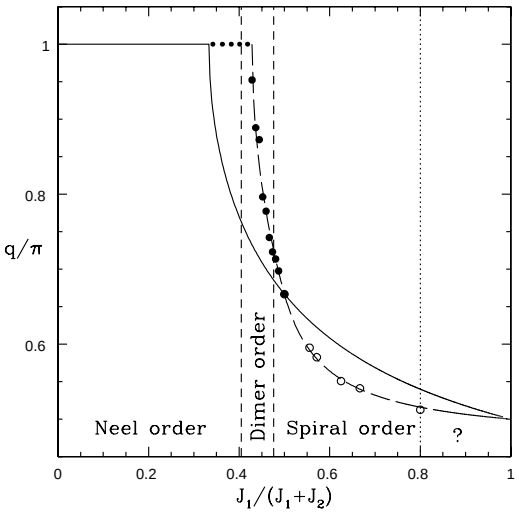

FIG. 2. Phase diagram of the model. The wavevector q is plotted as a function of $J_1/(J_1+J_2)$. The solid curve is the classical ordering wavevector, while the points are estimates of the location of the minimum triplet gap from both columnar dimer expansions (solid points) and diagonal dimer expansions (open points). The long dashed lines are the fit given in Eq. (16). The vertical short dashed lines indicate the region of spontaneously dimerized phase, and vertical dotted line indicate another possible transition point.

To determine whether the system is in the ordered phase, we need to compute the order parameter M defined by

$$M = \frac{1}{N} \sum_i \langle S_i^z \rangle \quad (7)$$

where the brackets denote ground-state expectation values. Actually, in this expansion, we can choose q different from that given in Eq. (2), the favored q should give a

lower energy. If $q = \pi$, we are expanding about the usual Neél phase.

Ising series have been calculated for the ground state energy per site, E_0/N, the order parameter M, and the triplet excitation spectrum (for the case of $q = \pi$ only) for several ratios of couplings x and (simultaneously) for several values of t up to order x^{10}. This calculation involves 116137 linked-clusters of up to 10 sites. The series for the case of $y = 1$ have been computed previously [5], and our results agree with these previous results. This is a highly non-trivial check on the correctness of the expansion coefficients, as the set of (anisotropic square-lattice) graphs considered here are completely different from the (triangular-lattice) graphs considered in Ref. [5] and the representation of the Hamiltonian as a Heisenberg-Ising model is also superficially different.

At the next stage of the analysis, we try to extrapolate the series to the isotropic point ($x = 1$) for those values of the exchange coupling parameters which lie within the ordered phase at $x = 1$. For this purpose, we first transform the series to a new variable

$$\delta = 1 - (1 - x)^{1/2} \ , \tag{8}$$

to remove the singularity at $x = 1$ predicted by the spin-wave theory. This was first proposed by Huse [21] and was also used in earlier work on the square lattice case [22]. We then use both integrated first-order inhomogeneous differential approximants [23] and Padé approximants to extrapolate the series to the isotropic point $\delta = 1$ ($x = 1$). The results of the Ising expansions will be presented in later sections.

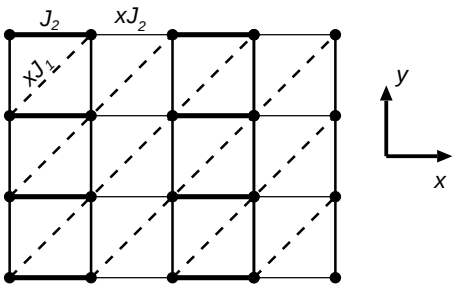

FIG. 3. Columnar dimerization pattern, the thick solid lines represent strongest bonds J_2, and thin solid lines and dashed lines represent weaker bonds xJ_2 and xJ_1, respectively. Note that the dimer centers lie on a rectangle lattice with spacing $2a$ in x-direction and a in y-direction. In characterizing the excitation spectrum we set the lattice spacing in both the x- and y-direction to be 1.

B. Dimer Expansions

For this system, we have carried out two types of dimer expansions corresponding to two types of dimer coverings. One is the columnar covering displayed in Fig. 3, and the other is the diagonal covering displayed in Fig. 4(a).

1. Columnar dimer expansions

In this expansion, we take the columnar bonds (D) denoted by the thick solid bonds in Fig. 3 as the unperturbed Hamiltonian H_0, and the rest of the bonds as perturbation, that is, we define the following "dimerized $J_1 - J_2$ model"

$$H = J_2 \sum_{(i,j)\in D} \mathbf{S}_i \cdot \mathbf{S}_j + x\Big[J_2 \sum_{(i,j)\notin D} \mathbf{S}_i \cdot \mathbf{S}_j + J_1 \sum_{\langle in\rangle} \mathbf{S}_i \cdot \mathbf{S}_j\Big] \tag{9}$$

We take the first term in above H as the unperturbed Hamiltonian, and the second term as perturbation. The unperturbed ground state is a product state of nearest neighbor singlet dimers and the perturbation couples these among themselves and with the pair-triplet states. At $x = 1$, one recovers the original Hamiltonian (1).

Two types of series can be obtained in this way. By fixing y, we can compute series in the single variable x up to order L,

$$E/J_2 = \sum_{i=0}^{L} c_i(y) x^i \tag{10}$$

In the other approach we keep both x and y as expansion parameters and obtain double series of the form

$$E/J_2 = \sum_{i=0}^{L} \sum_{j=0}^{i} d_{ij}(y)^i x^j \tag{11}$$

where the coefficients d_{ij} are computed up to order $i = L$.

The series has been computed up to order $L = 9$ for the ground-state energy E_0, and up to order $L = 8$ for the triplet excitation spectrum $\Delta(k_x, k_y)$. This calculation involves 49684 linked clusters of up to 9 sites.

Note that if the centers of the dimers are treated as lattice sites, one obtains a rectangular lattice with spacing $2a$ in x-direction and a in y-direction, where a is the lattice spacing of original lattice. In characterizing the excitation spectrum presented in the later sections we set the lattice spacing in both x- and y-directions to be 1. In this notation, the wavevector corresponding to the classical ordering is $(q - \pi, q)$, which varies from $(0, \pi)$ to $(-\pi/2, \pi/2)$ as J_1/J_2 increases from 0 to ∞.

The leading order series for the triplet excitation spectrum is:

$$\begin{aligned}\Delta(k_x, k_y)/J_2 = 1 + x[&-\tfrac{1}{2}\cos(k_x) + (1 - J_1/2J_2)\cos(k_y) \\ &-(J_1/2J_2)\cos(k_x + k_y)] + O(x^2)\end{aligned} \tag{12}$$

Note that the minimum of the above spectrum may not coincide with the ordering wavevector $(q-\pi, q)$ of the classical system.

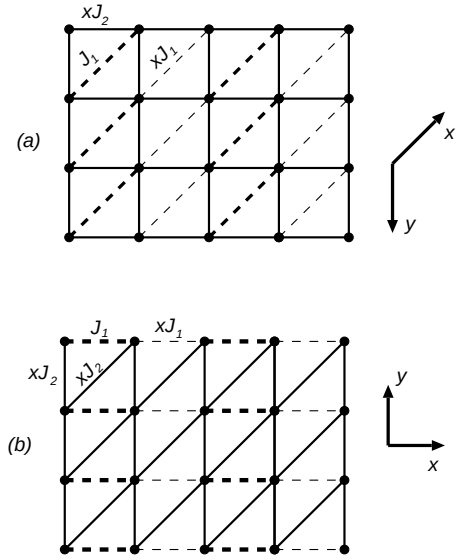

FIG. 4. (a) Diagonal dimerization pattern, the thick dashed lines represent strongest bonds J_1, and thin dashed lines and solid lines represent weaker bonds xJ_1 and xJ_2, respectively. (b) The equivalent lattice to (a) used in series expansions. Again note that the dimer centers lie on a rectangle lattice with spacing $2a$ in x-direction and a in y-direction. In characterizing the excitation spectrum we set the lattice spacing in both x- and y-direction to be 1.

2. Diagonal dimer expansions

In this expansion, we take the diagonal bonds (D) denoted by the thick dashed bonds in Fig. 4(a) as unperturbed Hamiltonian H_0, and rest of the bonds as perturbation. That is we define the following "dimerized J_1-J_2 model"

$$H = J_1 \sum_{(i,n)\in D} \mathbf{S}_i \cdot \mathbf{S}_j + x\Big[J_1 \sum_{(i,n)\notin D} \mathbf{S}_i \cdot \mathbf{S}_j + J_2 \sum_{\langle ij \rangle} \mathbf{S}_i \cdot \mathbf{S}_j\Big] \tag{13}$$

Again at $x = 1$, one recovers the original Hamiltonian (1).

For convenience, we have transformed the lattice shown in Fig. 4(a) to the equivalent one shown in Fig. 4(b). Again the dimer centers in Fig. 4(b) lie on a rectangular lattice with spacing $2a$ in x-direction and a in y-direction. In characterizing the excitation spectrum presented in the later sections we also set the lattice spacing in both x- and y-directions to be 1. In this representation the wavevector corresponding to the classical ordering is $(\pi-2q, q)$, which varies from $(-\pi, \pi)$ to $(0, \pi/2)$ as J_1/J_2 increases from 0 to ∞.

As in the case of columnar dimer expansions, two types of series have been computed up to order x^9 for the ground-state energy E_0, and up to order x^8 for the triplet excitation spectrum $\Delta(k_x, k_y)$. This calculation involves the same linked clusters as the columnar dimer expansions.

The leading order series for triplet excitation spectrum is

$$\Delta(k_x, k_y) = 1 + x[-\tfrac{1}{2}\cos(k_x) + (J_2/2J_1)\cos(k_y) - (J_2/2J_1)\cos(k_x + k_y)] + O(x^2) \tag{14}$$

Note that the minimum of Δ is at $(\pi - 2q, q)$, with q defined in Eq. (2), that is just the ordering wavevector of the classical system.

III. RESULTS

Having obtained the series for the various expansions above we present in this section the results of series analysis. We use integrated first-order inhomogeneous differential approximants [23] and Padé approximants to extrapolate the series.

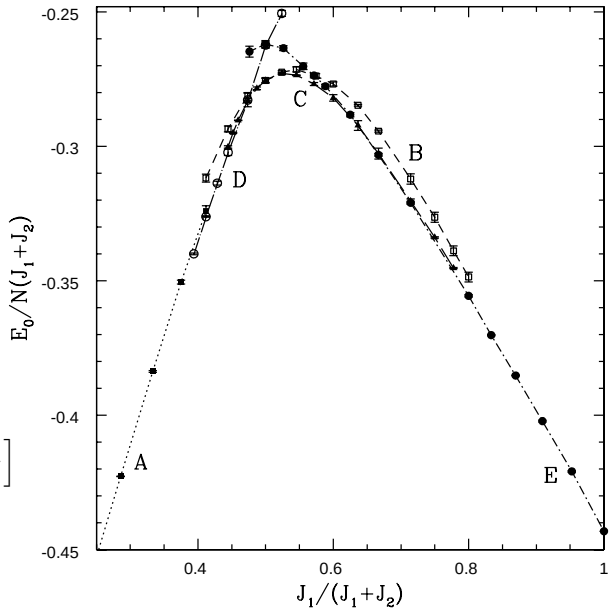

FIG. 5. The ground-state energy per site $E_0/N(J_1+J_2)$ as function of $J_1/(J_1+J_2)$, obtained from the Ising expansions about the Neél order (i.e. $q=\pi$) (A), the Ising expansions about the classical spiral order (i.e. $q \neq \pi$ defined by Eq. (2) (B), the Ising expansions using the q obtained by dimer expansions (C), the columnar dimer expansions (D) and the diagonal dimer expansion (E). The result at $J_2 = 0$ is the exact results for the ground state energy of a antiferromagnetic spin-chain [28].

A. Ground state energy

Fig. 5 shows the ground state energy per site E_0/N for the Hamiltonian in Eq. (1) obtained from various expansions, We see that the Ising expansions about the Neél order give the lowest energy and also show the best convergence in the region of $J_1/J_2 \lesssim 0.7$. The Ising expansions about the classical ground state (i.e. $q \neq \pi$ defined by Eq. (2)) gives the lowest energy in the region of $0.9 \lesssim J_1/J_2 \lesssim 1.2$, the columnar dimer expansions gives the lowest energy for $0.65 \lesssim J_1/J_2 \lesssim 0.9$, and the diagonal dimer expansions give the lowest energy for $J_1/J_2 \gtrsim 1.2$. Whenever the dimer expansions indicate an ordering wavevector different from the classical one, we have also computed the series expansion around the spiral-state with this modified wavevector. These always give lower ground state energies than those for the classical wavevector. Also, for $J_1/J_2 \gtrsim 1.2$, these modified Ising expansions lead to ground state energies that are almost identical with the diagonal dimer expansions.

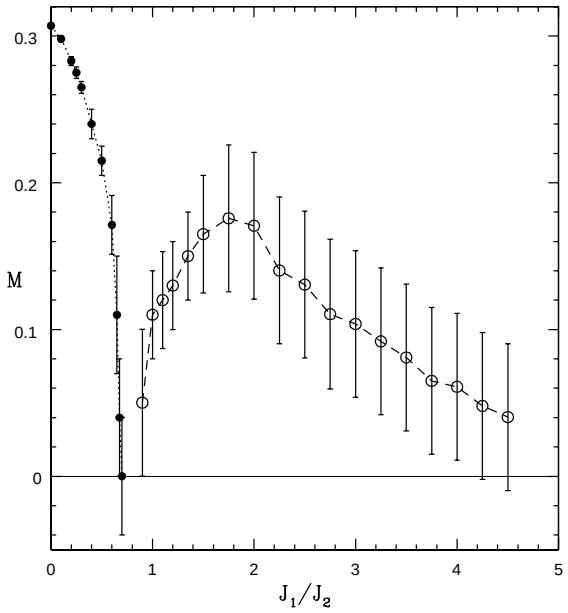

FIG. 6. The order parameter M *versus* J_1/J_2. The solid points with error bars are the estimates from the Ising expansions about Neél order (i.e. $q = \pi$) , while the open points are the estimates from Ising expansion about the classical spiral order (i.e., q defined by Eq. (2)).

B. Magnetisation

The order parameter M obtained from the Ising expansions about the classical ground state is shown in Fig. 6. The dependence on the amount of magnetic frustration is very similar to that obtained from linear spin wave theory. [24] The staggered magnetization associated with the Neél order exists up to $J_1/J_2 \simeq 0.7$, rather than up to $J_1/J_2 = 0.5$, as in the classical system. We can also see that the magnetisation M vanishes over the region $0.7 \lesssim J_1/J_2 \lesssim 0.9$, suggesting that this may belong to a quantum disordered phase. For $J_1/J_2 \gtrsim 0.9$, the system may have spiral order.

The fact that the Neél order survives beyond the classicaly stable region, is an example of promotion of collinear order by quantum fluctuations. A similar stabilization was found in the 1/4 depleted square-lattice Heisenberg model relevant to the material CaV_3O_7 by Kontani et al. [25] This can be viewed as a part of the more general phenomena of quantum order by disorder, [9] where quantum fluctuations help select and stabilize an appropriate type of order, typically collinear, in face of near classical degeneracy.

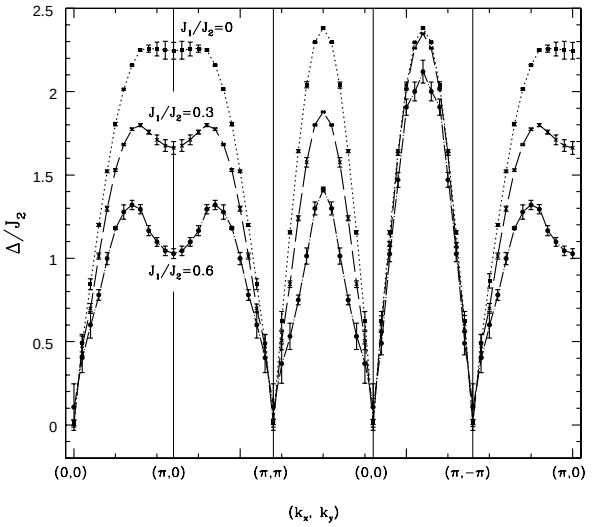

FIG. 7. Plot of triplet excitation spectra $\Delta(k_x, k_y)$ (derived from the Ising expansions about Neél order) along high-symmetry cuts through the Brillouin zone for coupling ratios $J_1/J_2 = 0, 0.3, 0.6$.

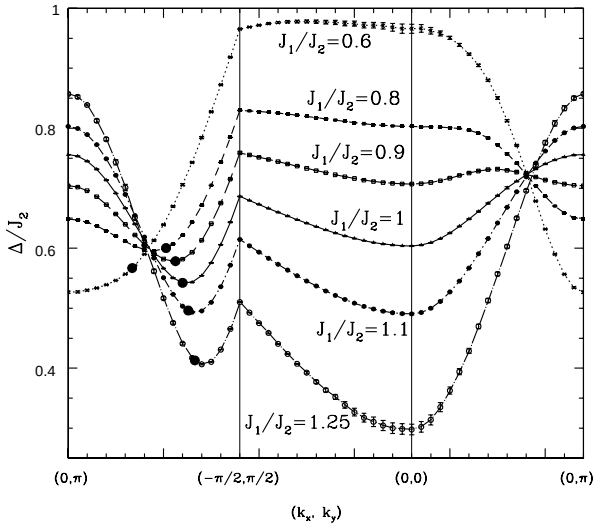

FIG. 8. Plot of triplet excitation spectrum $\Delta(k_x, k_y)$ for the columnar dimerized $J_1 - J_2$ model at $x = 0.5$ for coupling ratios $J_1/J_2 = 0.6, 0.8, 0.9, 1, 1.1, 1.25$. The big circles indicate the locations of classical ordering wavevectors.

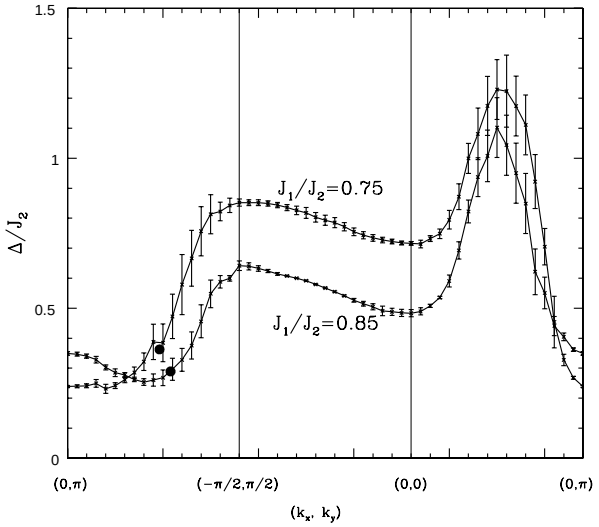

FIG. 9. Plot of triplet excitation spectrum $\Delta(k_x, k_y)$ derived from the columnar dimer expansions for the coupling ratios $J_1/J_2 = 0.75, 0.85$ and $x = 1$. The big full circles indicate the locations of classical ordering wavevector.

C. Triplet excitation spectrum

Fig. 7 shows the triplet excitation spectra $\Delta(k_x, k_y)$ for $J_1/J_2 = 0, 0.3, 0.6$ obtained from the Ising expansions about Neél order, where we can see the energy gap vanishes at (π, π) and its equivalent point.

We now present the spectra calculated from the columnar dimer expansions. We have previously noted that the leading order columnar dimer expansions give the minimum of the triplet excitation spectrum close to the classical ordering wavevector. Fig. 8 shows the triplet excitation spectra $\Delta(k_x, k_y)$ for the columnar dimerized $J_1 - J_2$ model at $x = 0.5$ and coupling ratios $J_1/J_2 = 0.6, 0.8, 0.9, 1, 1.1, 1.25$. It can be seen that the minimum gap is located at $(0, \pi)$ for $J_1/J_2 \lesssim 0.7$, or $(0, 0)$ for $J_1/J_2 \gtrsim 1.25$. For J_1/J_2 over the region $0.8 - 1.1$, the minimum is close to the classical ordering wavevector.

Extrapolating the columnar dimer series to $x = 1$ by the integrated differential approximants, one can get the triplet excitation spectra for the fairly narrow parameter range $0.7 \lesssim J_1/J_2 \lesssim 0.9$, and the results for $J_1/J_2 = 0.75$ and 0.85, are shown in Fig. 9. We find that the minimum gap is nonzero for these couplings. The minimum triplet gap as a function of J_1/J_2 are given in Fig. 10. We find that up to $J_1/J_2 \simeq 0.75$, the minimum gap is located at $(0, \pi)$, and for $J_1/J_2 \gtrsim 0.75$, the system is in an incommensurate phase, with the location of minimum gap given in Fig. 2.

The excitation spectra for the regime of small J_2/J_1 will be discussed in a later section.

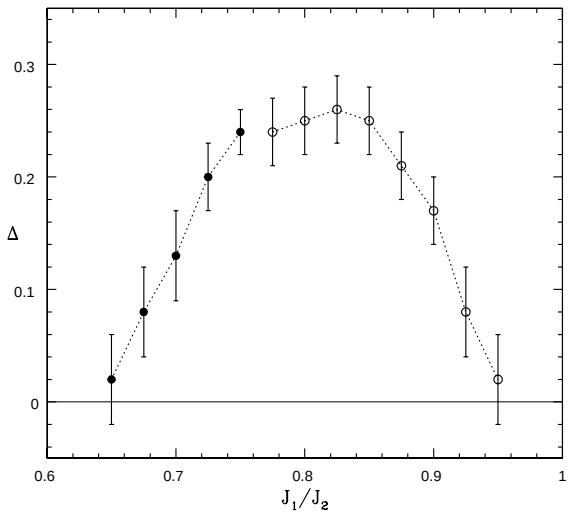

FIG. 10. The minimum triplet excitation gap Δ vs J_1/J_2 derived from the columnar dimer expansions. The full points indicate the minimum gap is located at $(0, \pi)$.

D. Phase Transitions and Critical Exponents

In this section we describe various estimations of the phase boundaries and the calculations of critical exponents associated with the transitions. We note that the estimates of critical exponents are not particularly accurate. The uncertainties shown are a measure of the spread among the Padé approximants. Given the short length of the series, they are best regarded as effective exponents.

First, combining the results of the Ising and the columnar dimer expansions, we estimate that Neél order disappears at $J_1/J_2 = 0.68(3)$. The phase adjacent to that appears to be spontaneously dimerized in the columnar pattern. This phase is analogous to the middle spontaneously dimerized phase in $J_{nn} - J_{nnn}$ square lattice model. [4] Our results are consistent with the transition from the Neél to the dimerized phase being a second-order transition, since, near the critical point, the ground state energy from the columnar dimer expansion matches very smoothly those from the Ising expansions. For a first-order transition, there should be a discontinuity in the slope at the transition. Similarly, we estimate the transition point between spontaneously dimerized phase and the spiral phase to be at $J_1/J_2 = 0.91(3)$.

Phase boundaries for the columnar dimerized Hamiltonian can be more fully studied by the columnar dimer expansions. By applying the Dlog Padé approximants to the triplet series at the wavevector of the minimum gap, we can locate the critical points at which the gap closes. The results are presented in Fig. 11, where in our analysis we have assumed that the minimum gap is located at the classical ordering wavevector for J_1/J_2 in the range $0.8 - 1.2$. The associated critical exponent ν is about 0.8(1), with not much variation with J_1/J_2. It would be interesting to calculate the spectral weight for the triplet excitations to see if they vanish, suggesting the appearance of spinon excitations. [14] These results are not accurate enough to decide if the transitions belong to the O(3) nonlinear sigma model universality class ($\nu = 0.70$) [26] or the O(4) exponents associated with the SO(3) nonlinear sigma model ($\nu = 0.74$) [15,27]. For J_1/J_2 in the region $0.7 - 0.9$, we find critical points x_c larger than unity. This is evidence that this phase is spontaneously dimerized.

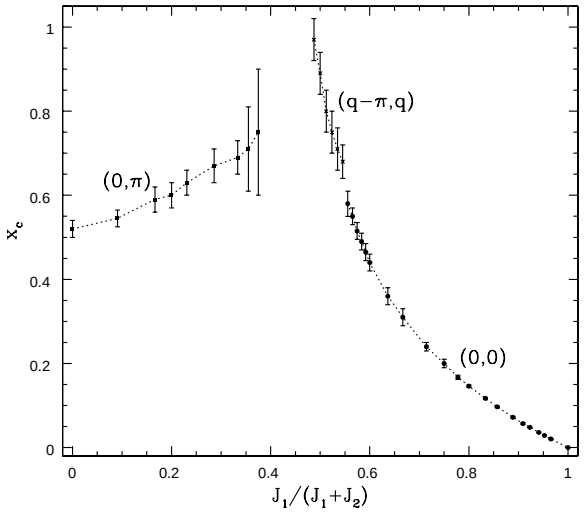

FIG. 11. The critical point x_c as a function of $J_1/(J_1 + J_2)$ as obtained from Dlog Padé approximants to the minimum energy gap of columnar dimer expansions. The locations of minimum gap are $(0, \pi)$ for $J_1/J_2 \lesssim 0.6$, or near classical ordering wavevector $(q - \pi, q)$ for $0.95 \lesssim J_1/J_2 \lesssim 1.2$, or (0,0) for $J_1/J_2 \gtrsim 1.25$.

For diagonal dimer expansions, we can also get the phase boundary by using the Dlog Padé approximants to locate the critical points where the gap vanishes. The results are shown in Fig. 12. The associated critical exponent ν is found to be approximately 0.75(10), and also does not vary much with J_2/J_1. For $J_2/J_1 \gtrsim 1.75$ the minimum of the energy gap is clearly $(-\pi, \pi)$, which is the classical ordering wavevector.

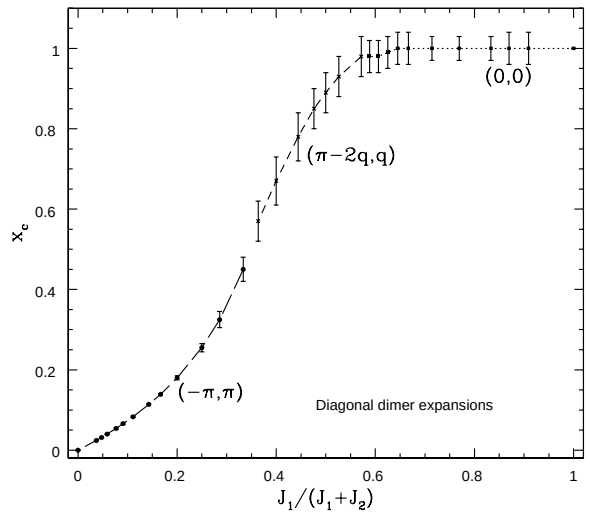

FIG. 12. The critical point x_c as a function of $J_1/(J_1+J_2)$ as obtained from Dlog Padé approximants to the minimum energy gap of diagonal dimer expansions. The locations of minimum gap are $(0,0)$ for $J_2/J_1 \lesssim 0.75$, or near classical ordering wavevector $(\pi-2q,q)$ for $0.75 \lesssim J_2/J_1 \lesssim 1.75$, or $(-\pi,\pi)$ for $J_2/J_1 \gtrsim 1.75$.

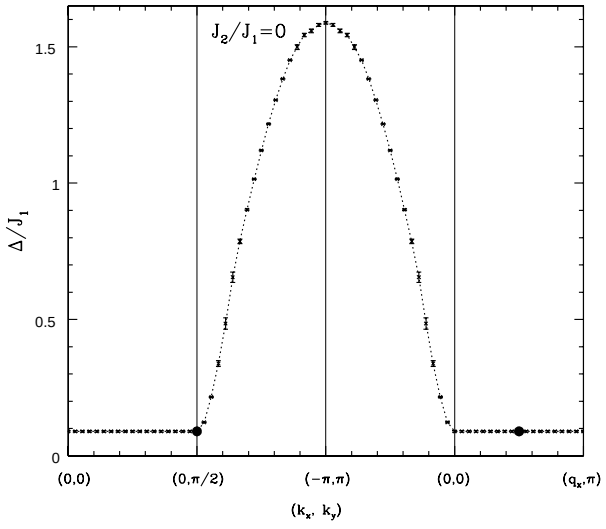

FIG. 13. Plot of triplet excitation spectrum $\Delta(k_x,k_y)$ along selected contours in Brillouin zone (derived from the diagonal dimer expansions) for coupling ratios $J_2/J_1=0$. The big full circle indicates the position of the classical ordering wavevector and $q_x=\pi(\pi-2q)/q=0$ for $J_2/J_1=0$.

E. Weakly Coupled Zig-Zag Chains

In this section we discuss the excitation spectra for small J_2/J_1, when the system can be thought of as weakly coupled spin-chains. The coupling between the chains is frustrated, and has been called zig-zag coupling in the literature.

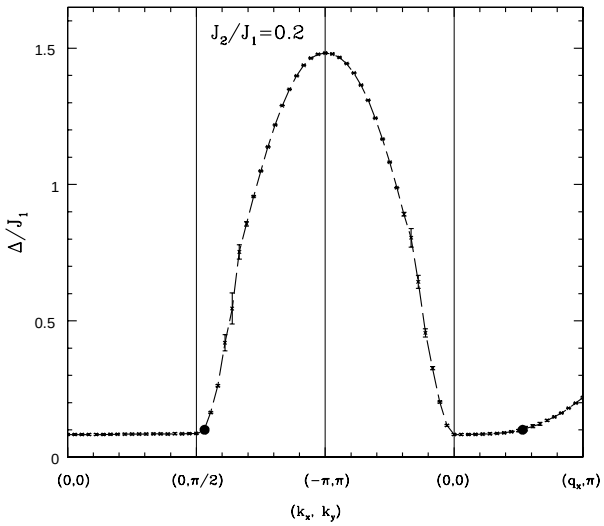

FIG. 14. Plot of triplet excitation spectrum $\Delta(k_x,k_y)$ along selected contours in Brillouin zone (derived from the diagonal dimer expansions) for coupling ratios $J_2/J_1=0.2$. The big full circle indicates the position of the classical ordering wavevector and $q_x=\pi(\pi-2q)/q=-0.12\pi$ for $J_2/J_1=0.2$.

For small values of J_2/J_1, the critical points in the diagonal dimer expansions lie very close to unity, and it is very difficult to locate the wavevector of the gap minimum at $x=1$. Fig. 13 gives the dispersion at $x=1$ for the case $J_2=0$ (i.e., decoupled spin chains). Here we get a small but nonzero minimum gap, due to the fact that we have not taken into account the singular behavior of the spin-chain. This can be done by extrapolating the series in a new variable

$$\delta = 1-(1-x)^{2/3}, \tag{15}$$

in which case the gap does vanish. For J_2 non-zero, we do not know if $x=1$ is gapped or critical, and hence do not know which extrapolation variable to use. For simplicity, we discuss primarily an extrapolation in the original variable, which assumes there is no singularity at $x=1$. Note, however, that even with this extrapolation we do get a flat dispersion between $(0,0)$ and $(0,\pi/2)$, as expected. As we increase J_2/J_1 (up to $J_2/J_1 \simeq 0.2$), we still get a very flat dispersion over the region $(0,0)$ and $(0,\pi/2)$. The gap over this region is also very small (similar to that for $J_2=0$), and in fact it is zero within errorbars if we extrapolate the series using the variable

δ. As an example, the dispersion is shown in Fig. 14 for $J_2/J_1 = 0.2$ (extrapolated assuming no critical points for $x < 1$). At larger values of J_2/J_1, for example for $J_2/J_1 = 0.5$, the dispersion is more pronounced and is shown in Fig. 15. We can see that the position of the minimum gap is not located exactly at the classical ordering wavevector, but deviates from it along the direction connecting $(0, \pi/2)$ and $(-\pi, \pi)$. This location of the minimum gap is plotted in Fig. 2.

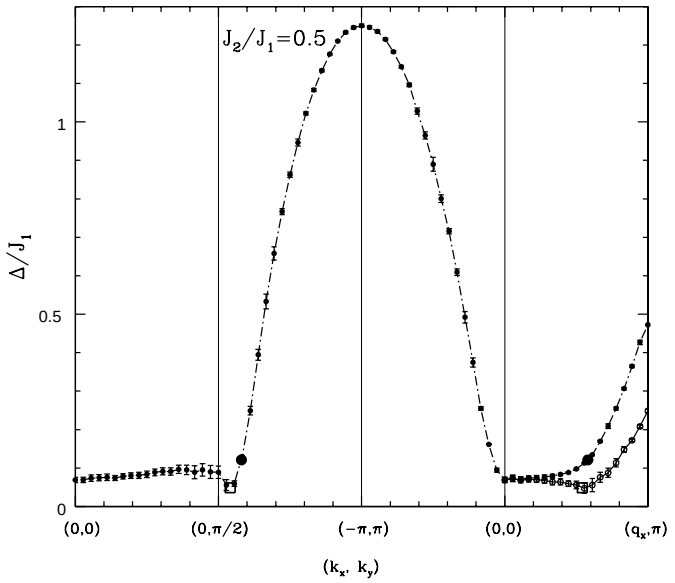

FIG. 15. Plot of triplet excitation spectrum $\Delta(k_x, k_y)$ along selected contours in Brillouin zone (derived from the diagonal dimer expansions) for coupling ratios $J_2/J_1 = 0.5$. The big full point indicates the position of classical ordering wavevector, while the big open square indicates the position of minimum gap. The solid (open) points in rightmost windows are spectra along contour connecting $(0, 0)$ and the classical ordering wavevector (the position of minimum gap) by a straight line up to $k_y = \pi$.

The wavevector q obtained from both columnar dimer expansions and diagonal dimer expansions can be fitted very well by the simple form:

$$q = \begin{cases} \arccos[-(3J_2/J_1 - 2)/2], & 0.75 \gtrsim J_1/J_2 \leq 1; \\ \arccos\{-[2(3J_1/J_2 - 2)]^{-1}\}, & J_1/J_2 \geq 1. \end{cases} \tag{16}$$

which is shown by a dashed lined in Fig. 2.

Using the above results for q, we can obtain more reliable results for the ground state energy by the Ising expansion, and the results are shown in Fig. 5. The results for the magnetisation M obtained using this wavevector agree (within errorbars) with the results obtained using the classical wavevector, shown in Fig. 6 and, hence, are not shown.

IV. CONCLUSIONS

In this paper we have studied a class of Heisenberg models, which interpolate between the square-lattice, the triangular-lattice and the linear-chain models. As discussed in the introduction, these models should describe the magnetic properties of the insulating phase of a range of layered organic superconductors. Furthermore, using uniaxial stress it may be possible to vary the parameter J_1/J_2 and induce some of the quantum phase transitions considered in this paper. We find that the model has a particulary rich phase diagram: Neél, spiral, dimerized, and possible critical phases occur. Except, perhaps, for the region of weakly coupled chains the phase diagram is rather well determined by our series expansions, and it would be difficult for any other numerical method to have comparable accuracy. Some of the most notable features are that the two-sublattice Neél phase appears stable beyond its classical regime of stability and in the spiral phase, the ordering wavevector is different from the classical ordering wavevector except for the case of the triangular-lattice Heisenberg model. The region of weakly coupled chains is nearly critical. In studying the instability of the dimerized phase to the spiral phase, the critical exponents for various dimer expansions give values of ν in the range $0.65 < \nu < 0.9$ which is consistent with either $O(4)$ or $O(3)$ universality class. This, as well as the possibility of spinon excitations in the quantum disordered phases of this model, deserve further attention.

ACKNOWLEDGMENTS

This work is supported in part by a grant from the National Science Foundation (DMR-9616574) (R.R.P.S), the Gordon Godfrey Bequest for Theoretical Physics at the University of NSW, and by the Australian Research Council (Z.W. and R.M.). The computation has been performed on Silicon Graphics Power Challenge and Convex machines. We thank the New South Wales Centre for Parallel Computing for facilities and assistance with the calculations. We thank J. Merino, J. Oitmaa, C.J. Hamer and S. Sachdev for helpful discussions. We thank C.J. Hamer and J. Oitmaa for providing some of the computer codes we used.

* e-mail address: w.zheng@unsw.edu.au
† e-mail address: ross@newt.unsw.edu.au
‡ e-mail address: rrpsing@ucdavis.edu

[1] S. Chakravarty, B. I. Halperin and J. Ye, Phys. Rev. B **39**, 2344 (1989); A. V. Chubukov, S. Sachdev and J. Ye, Phys. Rev. B **49**, 11919 (1994).
[2] A. Auerbach, *Interacting Electrons and Quantum Magnetism*, (Springer - Verlag, New York, 1994).
[3] S. Sachdev, in *Low Dimensional Quantum Field Theories for Condensed Matter Physicists,* edited by Y. Lu, S. Lundqvist, and G. Morandi, (World Scientific, Singapore, 1995).
[4] H. J. Schulz, T. A. L. Ziman, and D. Poilblanc, J. Phys. I France **6**, 675 (1996); J. Oitmaa and Z. Weihong, Phys. Rev. B **54**, 3022 (1996), and references therein; O. Sushkov, Zheng Weihong, V.N. Kotov, and J. Oitmaa, unpublished.
[5] R.R.P. Singh and D.A. Huse, Phys. Rev. Lett., **68**, 1766 (1992).
[6] P. Lecheminant et al, Phys. Rev. B**56**, 2521 (1997).
[7] N. Elstner and A. P. Young, Phys. Rev. B**50**, 6871 (1994).
[8] R. R. P. Singh, O. A. Starykh and P. J. Freitas, J. Appl. Phys. **83**, 7387 (1998).
[9] P. Chandra, P. Coleman, and A. I. Larkin, J. Phys.: Condens. Matter **2**, 7933 (1990).
[10] R. H. McKenzie, cond-mat/9802198, to appear in *Comments on Condensed Matter Physics*.
[11] For an example of uniaxial experiments on these materials see, C. E. Campos *et al.*, Physica B **211**, 293 (1995).
[12] J. Schmalian, Phys. Rev. Lett. **81**, 4232 (1998); H. Kino and H. Kontani, cond-mat/9807147; H. Kondo and T. Moriya, cond-mat/9807322; M. Votja and E. Dagotto, cond-mat/9807168, to appear in Phys. Rev. B; K. Kuroki and H. Aoki, cond-mat/9812026.
[13] S. R. White and I. Affleck, Phys. Rev. B **54**, 9862 (1996), and references therein.
[14] R. R. P. Singh and N. Elstner, Phys. Rev. Lett. **81**, 4732 (1998); R. R. P Singh and Z. Weihong, cond-mat/9811028.
[15] A. V. Chubukov, S. Sachdev, and T. Senthil, Nucl. Phys. B **426**, 601 (1994).
[16] A. Angelucci, Phys. Rev. B **44**, 6849 (1991); ibid. **45**, 5387 (1992).
[17] N. Read and S. Sachdev, Phys. Rev. Lett. **66**, 1773 (1991).
[18] H.X. He, C.J. Hamer and J. Oitmaa, J. Phys. A **23**, 1775 (1990).
[19] M. P. Gelfand, R.R.P. Singh, and D.A. Huse, J. Stat. Phys. **59**, 1093 (1990).
[20] M. P. Gelfand, Solid State Commun. **98**, 11 (1996).
[21] D.A. Huse, Phys. Rev. B **37**, 2380 (1988).
[22] W.H. Zheng, J. Oitmaa and C.J. Hamer, Phys. Rev. B **43**, 8321 (1991).
[23] A.J. Guttmann, in "Phase Transitions and Critical Phenomena", Vol. 13 ed. C. Domb and J. Lebowitz (New York, Academic, 1989).
[24] J. Merino, unpublished.
[25] H. Kontani, M. E. Zhitomirsky, and K. Ueda, J. Phys. Soc. Jap. **65**, 1566 (1996).
[26] J. C. Le Guillou and J. Zinn-Justin, Phys. Rev. Lett. **39**, 95 (1977).
[27] P. Azaria, B. Delamotte, and T. Jolicoeur, Phys. Rev. Lett. **64**, 3175 (1990); P. Azaria, B. Delamotte, and D. Mouhanna, ibid. **68**, 1762 (1992).
[28] H.A. Bethe, Z. Phys. **71**, 205 (1931).